



Supplement of

Importance of multiple sources of iron for the upper-ocean biogeochemistry over the northern Indian Ocean

Priyanka Banerjee

Correspondence to: Priyanka Banerjee (pbanerjee@iisc.ac.in)

The copyright of individual parts of the supplement might differ from the article licence.

Supplementary Information

Table S1. Magnitude of bias in CESM simulated DFe concentration (nM)

REGION	BIAS
5°S-20°S LATITUDE	0.16
5°S-30°N LATITUDE	0.47
ARABIAN SEA (WEST OF 60°E LONGITUDE)	-0.07
OPEN OCEAN (DEPTH > 1000 M)	0.38
COASTAL REGIONS (DEPTH < 1000 M)	0.32

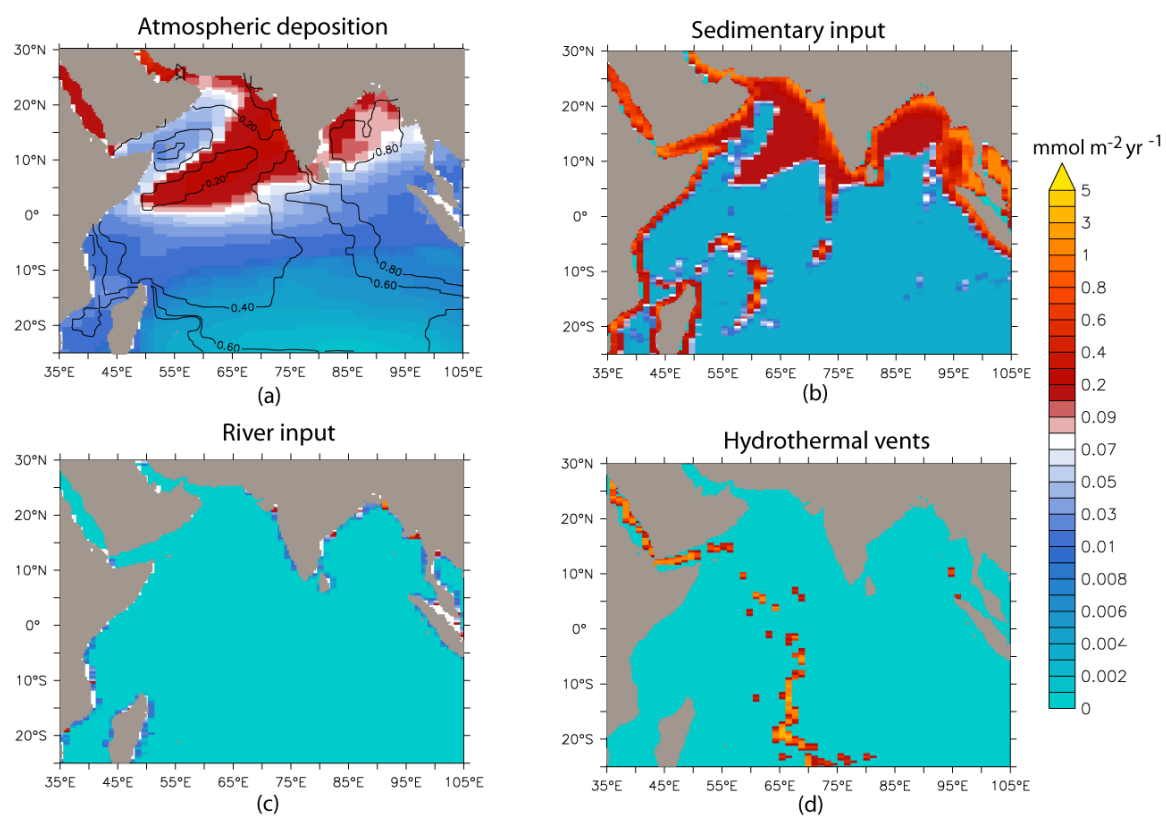


Fig. S1 Iron fluxes from the various sources considered in CESM-MARBL over the northern Indian Ocean. Contours in (a) show the fractional contribution of black carbon to atmospheric iron flux.

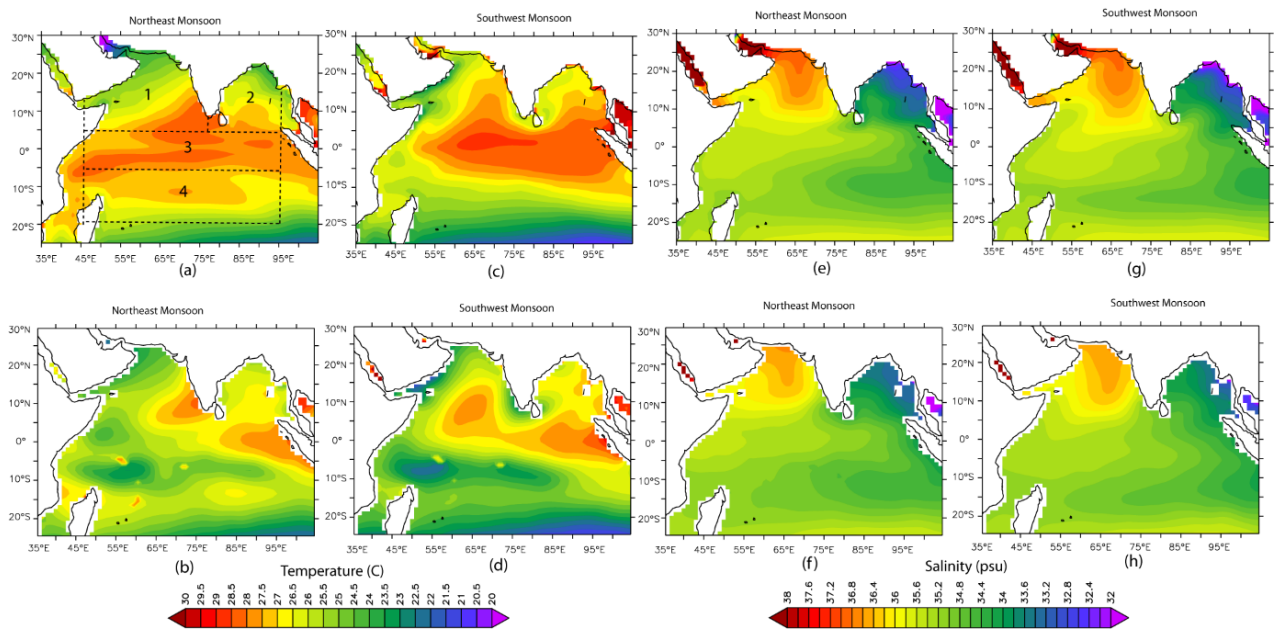


Fig. S2 Comparison of (a-d) temperature and (e-h) salinity simulated by CESM (upper panels) with (lower panels) World Ocean Atlas 2018 data averaged over the upper 100 m. In (a) the regions marked (1), (2), (3) and (4) are Arabian Sea (AS), Bay of Bengal (BoB), the equatorial Indian Ocean (EQIO), and the southern tropical Indian Ocean (STIO) respectively. These regions are used in Figures S3, S4, S7 and S8.

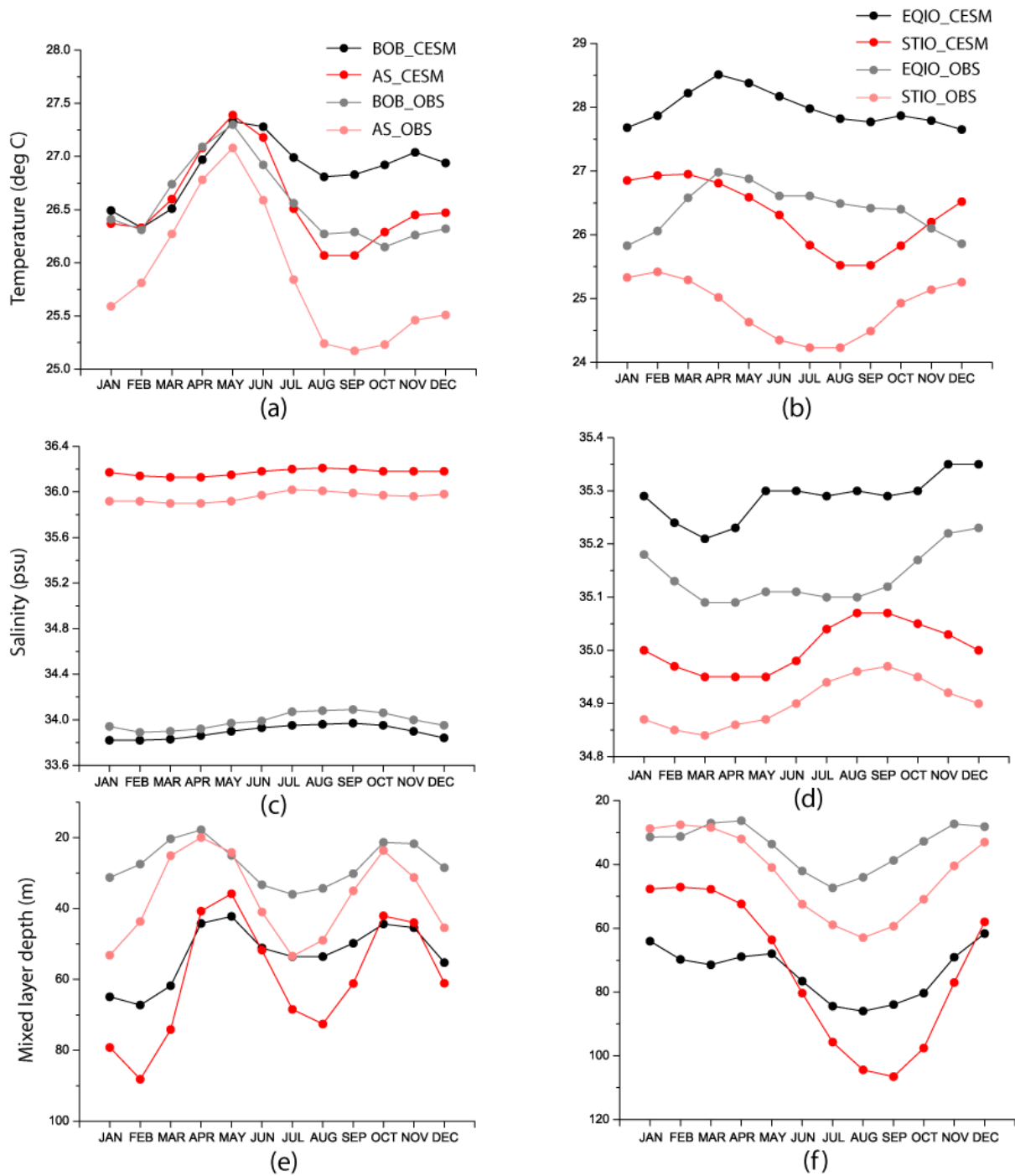


Fig. S3 Seasonal cycle of evolution of (a and b) temperature, (c and d) salinity and (e and f) mixed layer depth from CESM simulations and observation data for (left panels) the AS and the BoB and (right panels) the EQIO, and the STIO. Temperature and salinity are averaged over upper 100 m. For observation data, temperature and salinity are obtained from World Ocean Atlas 2018 and mixed layer depth is derived from Argo floats (Holte et al., 2017).

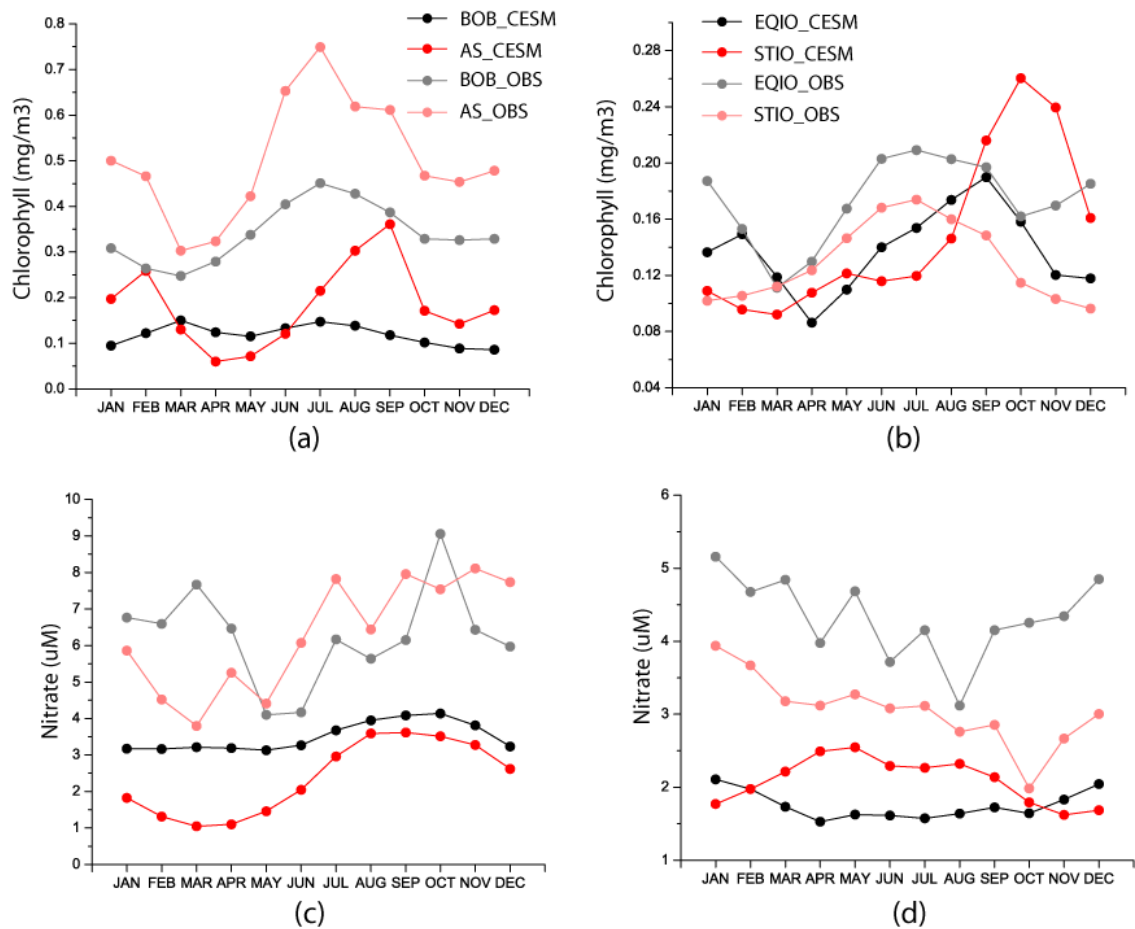


Fig. S4 Seasonal cycle of **(a and b)** surface chlorophyll concentration and **(c and d)** upper 100 m nitrate concentrations from CESM simulations and observations for (left panels) the AS and the BoB and (right panels) the EQIO, and STIO. For observation data, surface chlorophyll concentration is from OC-CCI and nitrate is from World Ocean Atlas 2018.

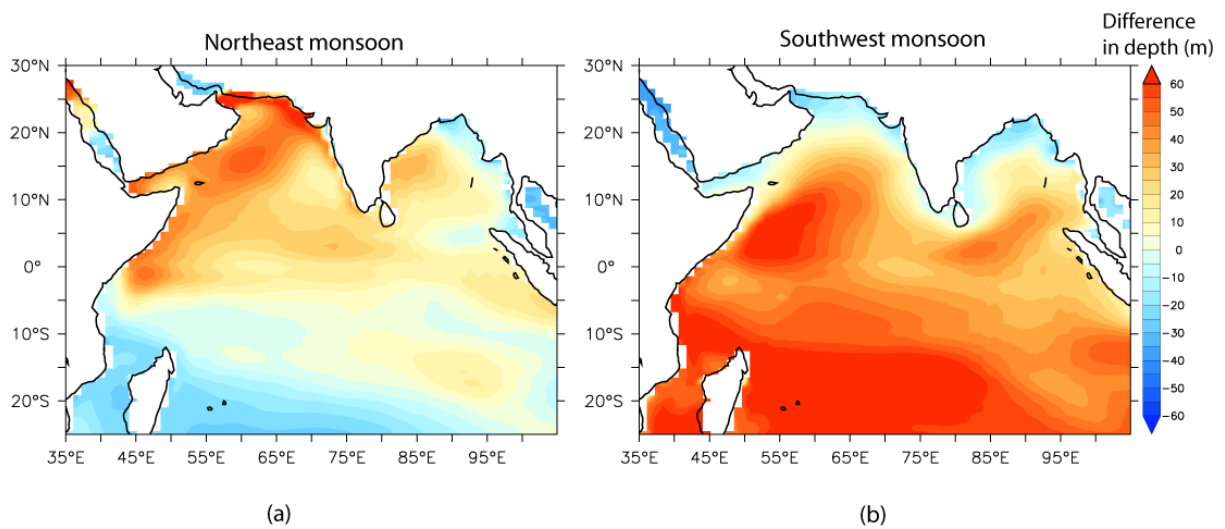


Fig. S5 Differences between CESM-simulated mixed layer depth and the depth of the isolume $0.415 \text{ mol quanta m}^{-2} \text{ day}^{-1}$ ($Z_{0.145}$). Positive values encompass the regions having deeper mixed layer compared to $Z_{0.145}$, and, thereby, indicates the regions which potentially experiences light limitation of primary productivity.

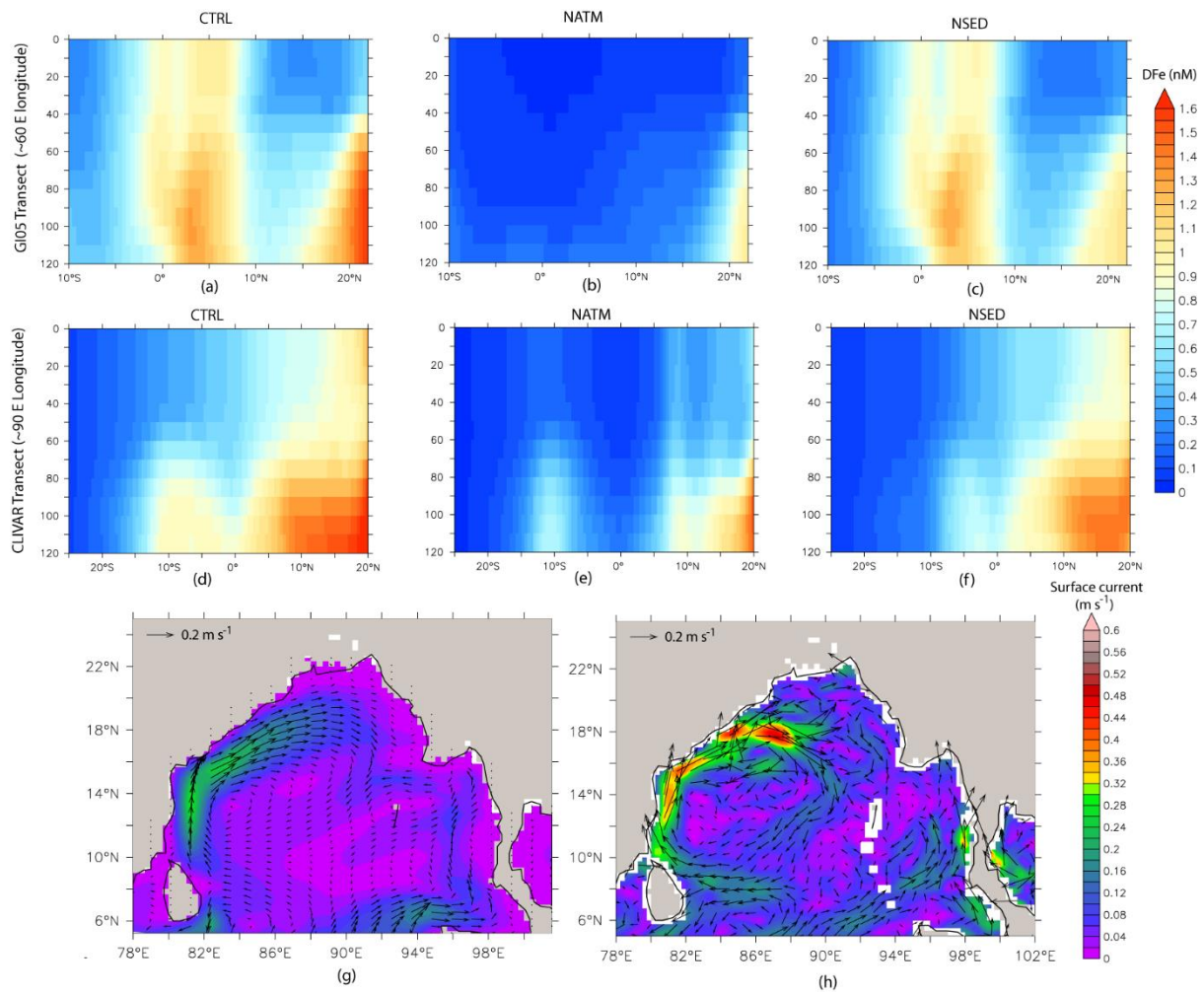


Fig. S6 Vertical variation in DFe along (a-c) GI05 and (d-f) CLIVAR transects for CTRL, NATM and NSED cases. (g-h) Surface currents over the Bay of Bengal for the month of April, from (g) CESM simulations and (h) OSCAR retrievals.

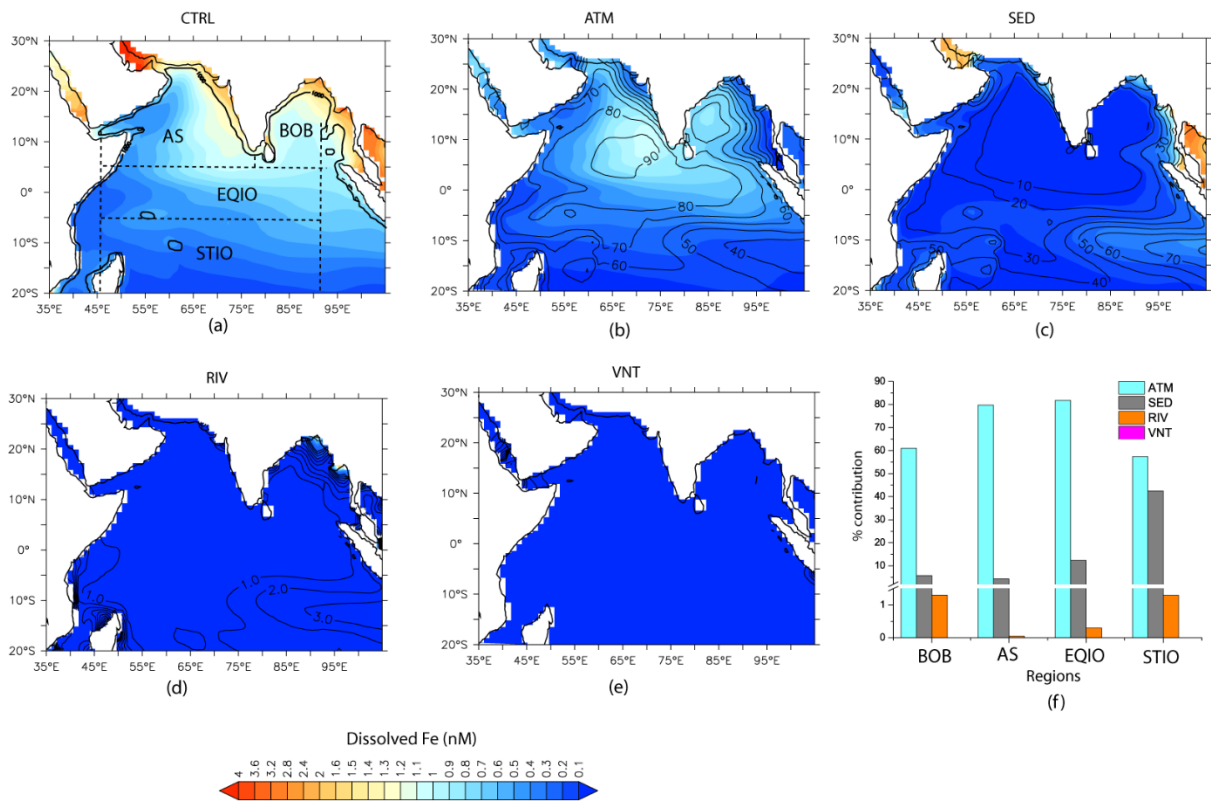


Fig. S7 Contribution of different sources of DFe during northeast monsoon season to total DFe concentrations averaged over the upper 100 m. Shading in (a) shows total DFe concentration when all sources are included and shadings in (b-e) shows DFe concentrations associated with a specific source. Contours in (b-e) are the percentage contribution of a specific source to the total DFe concentrations. (f) bar chart depicting source-specific DFe contribution (in %) over the BoB, the AS, the EQIO and the STIO. These regions are marked by the dashed boxes in (a). The thick black contour in (a) traces the 1000 m bathymetry.

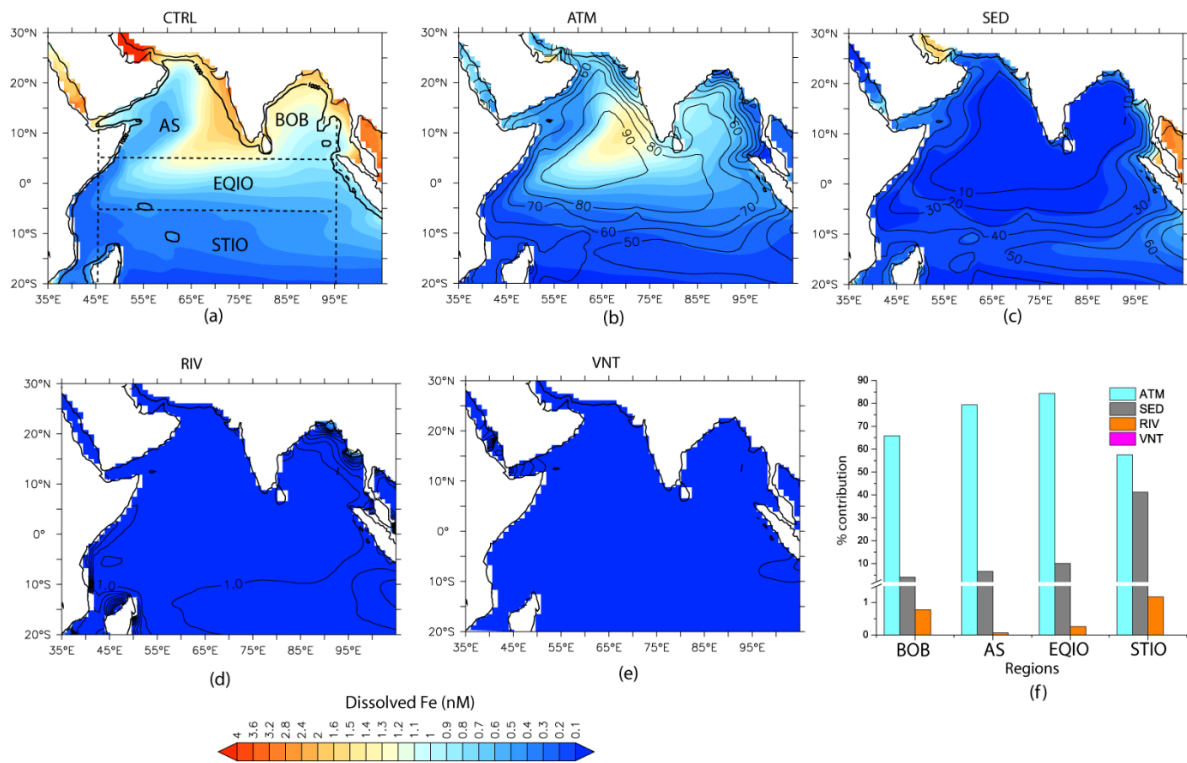


Fig. S8 Same as Figure S7 but for southwest monsoon season.

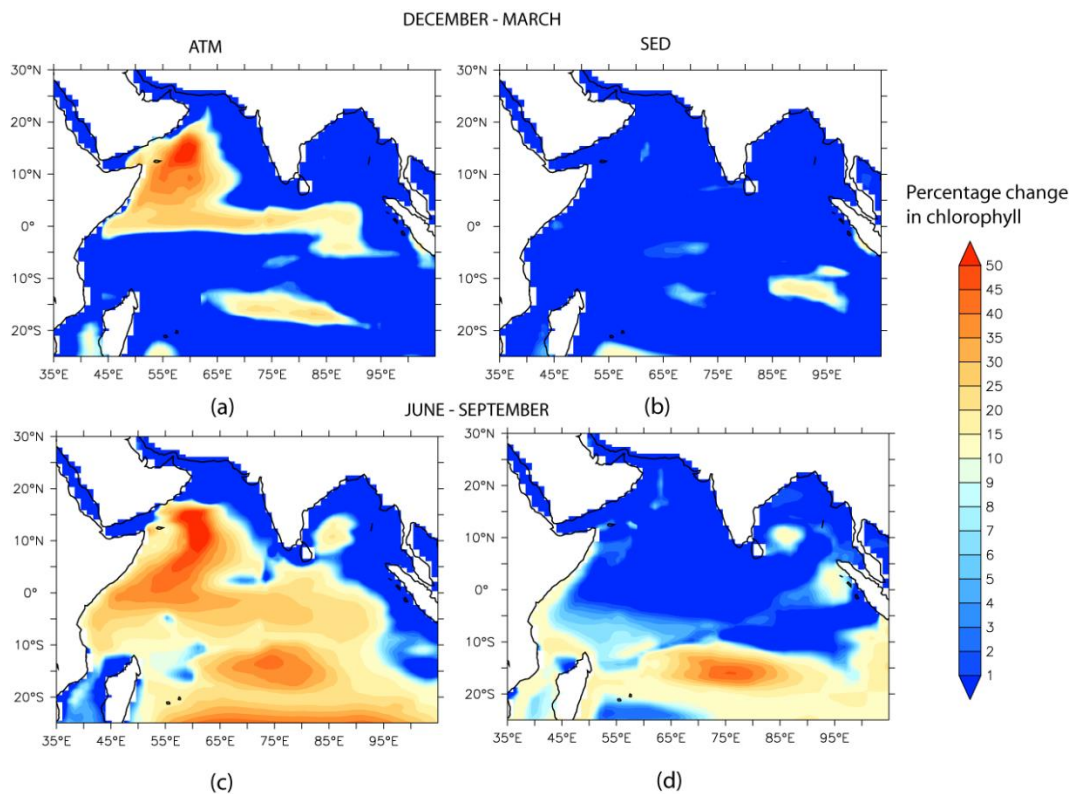


Fig. S9 Shading shows the percentage contribution of (a and c) atmospheric and (b and d) sedimentary sources of DFe during the (a and b) northeast monsoon and the (c and d) southwest monsoon months to surface chlorophyll concentrations.

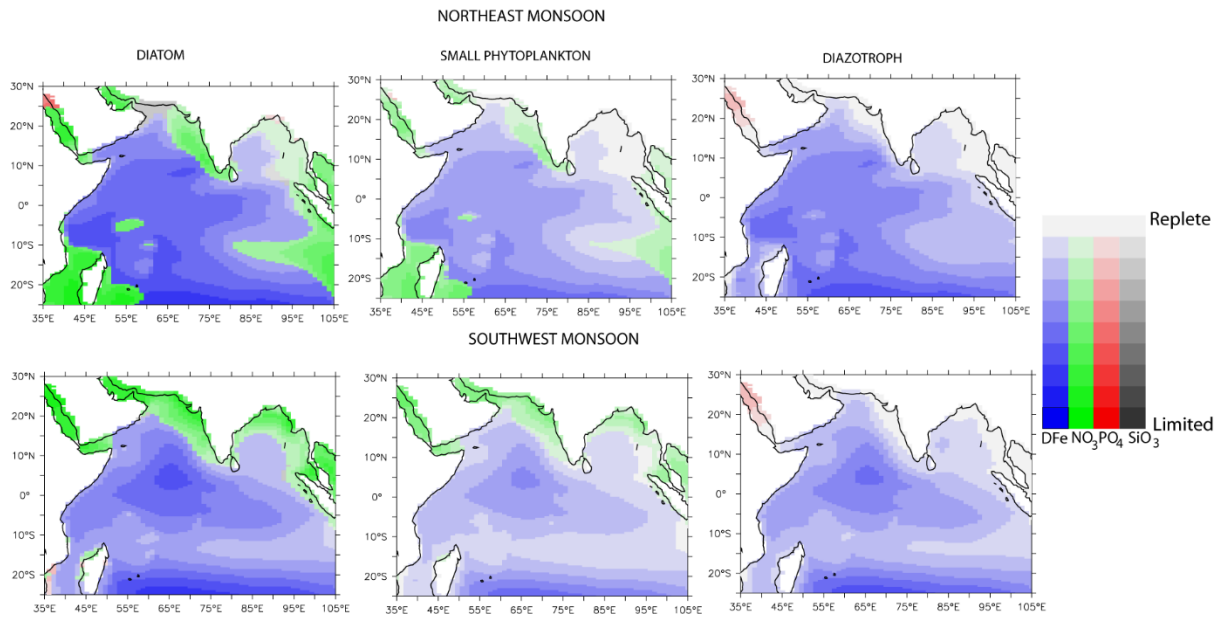


Fig. S10 Spatial pattern of surface nutrient limitations for different phytoplankton functional types from NATM simulation. Green: nitrate, blue: iron, red: phosphate and grey: silicate limitations.

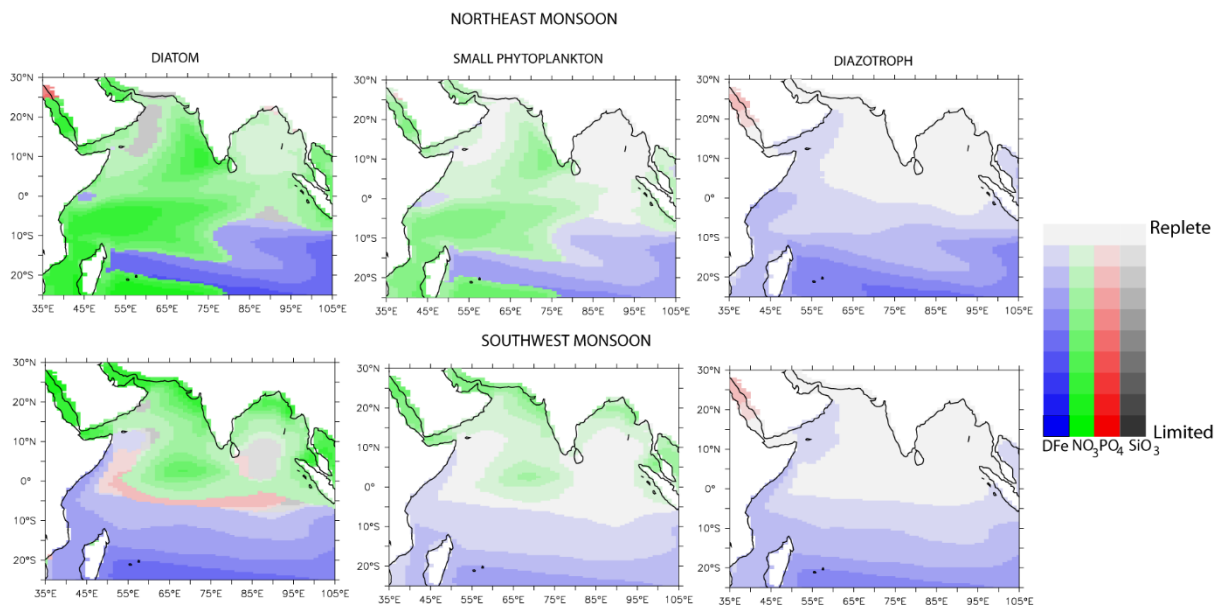


Fig. S11 Same as Figure S10 but for NSED simulations.

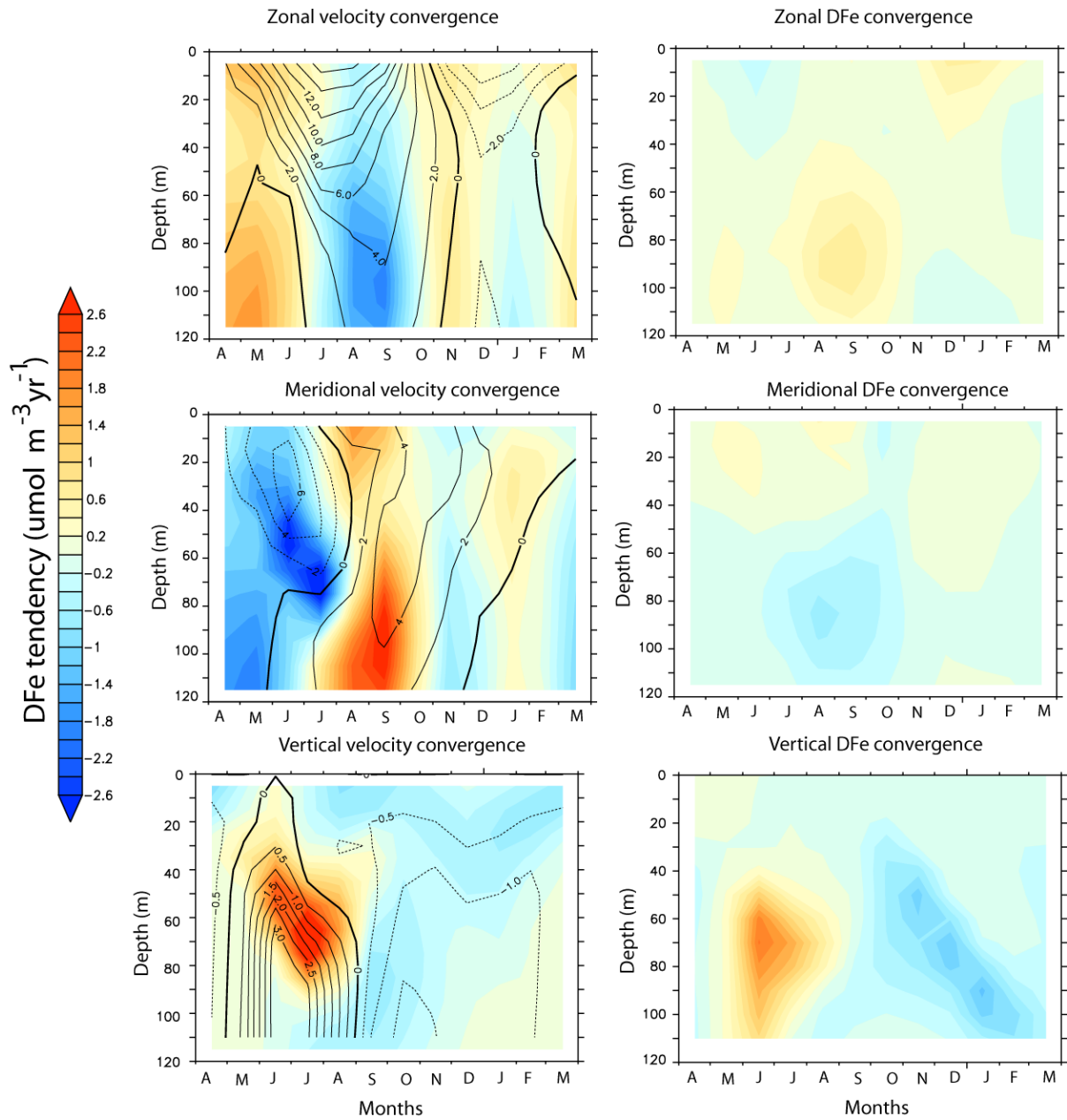


Fig. S12 Shading show DFe tendency in the western AS due to (left panels) velocity convergence and (right panels) tracer convergence. The contours in the upper to lower panels are the zonal, meridional, and vertical velocity (in m s^{-1}) respectively. Continuous contours are for positive values and dashed contours are for the negative values of the velocity components. The contour intervals are not uniform between different panels. Note that the vertical velocity has been multiplied by 5000.

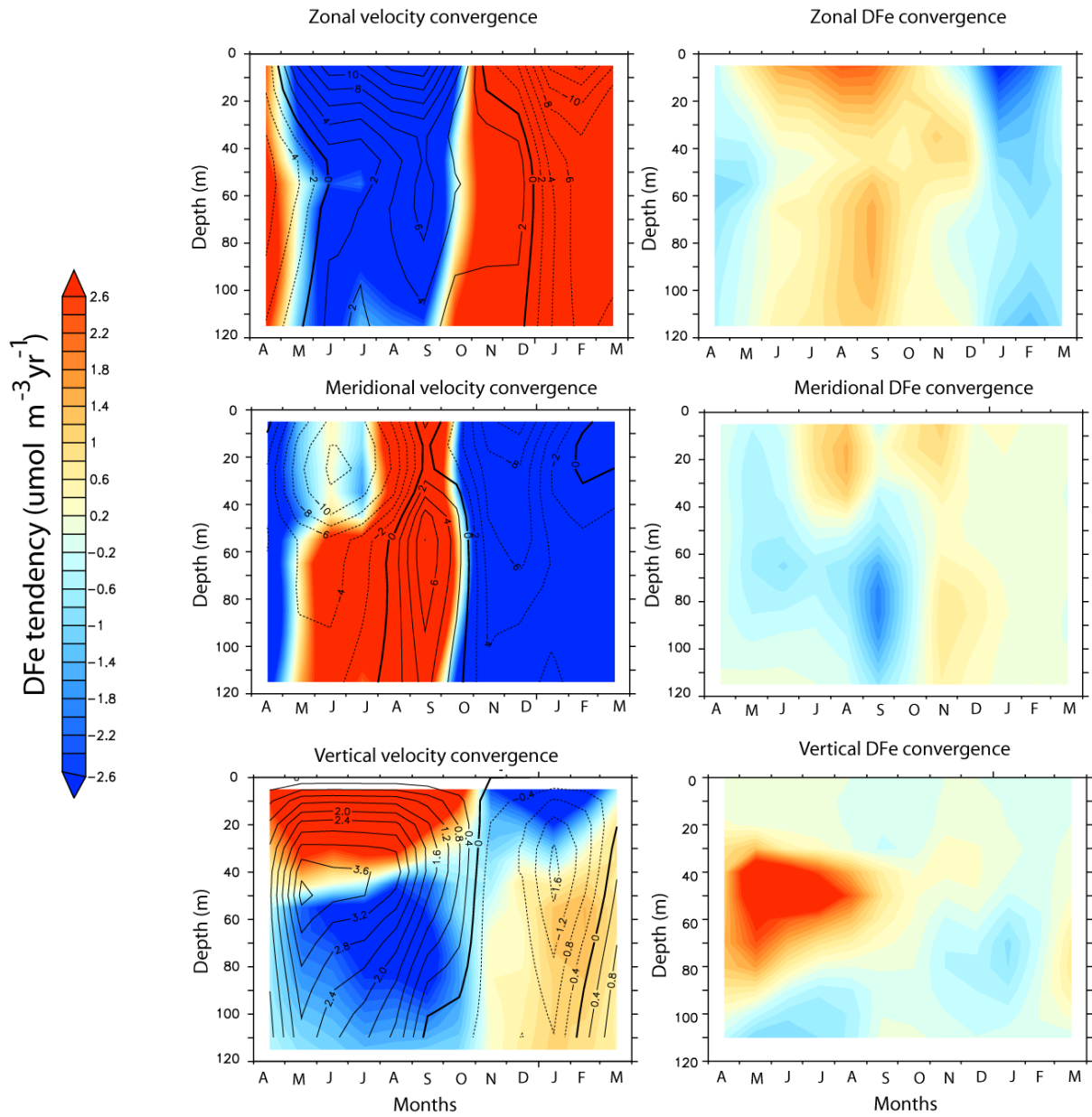


Fig. S13 Same as Figure S12 but for the southern BoB.

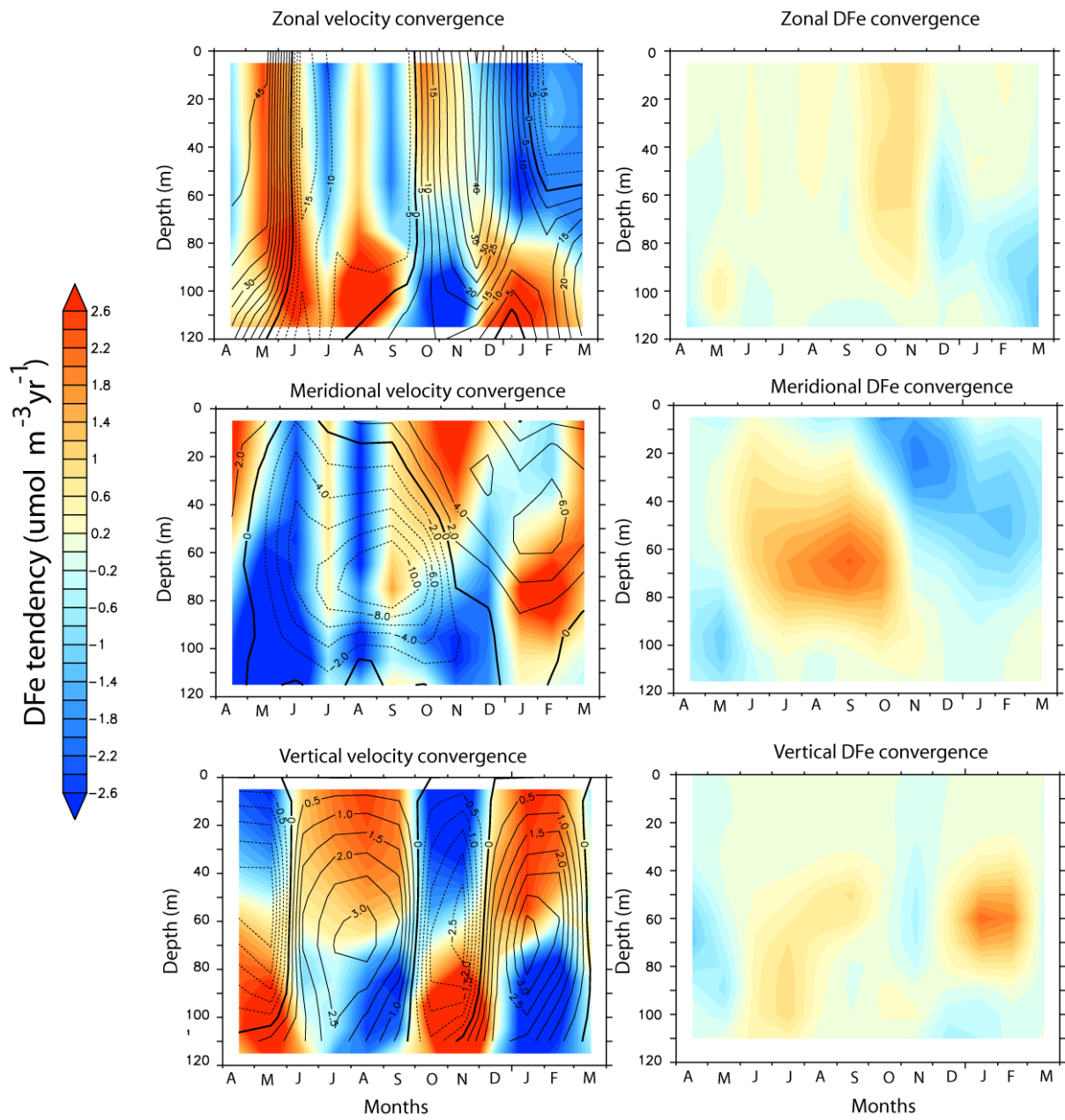


Fig. S14 Same as Figure S12 but for the central equatorial IO.

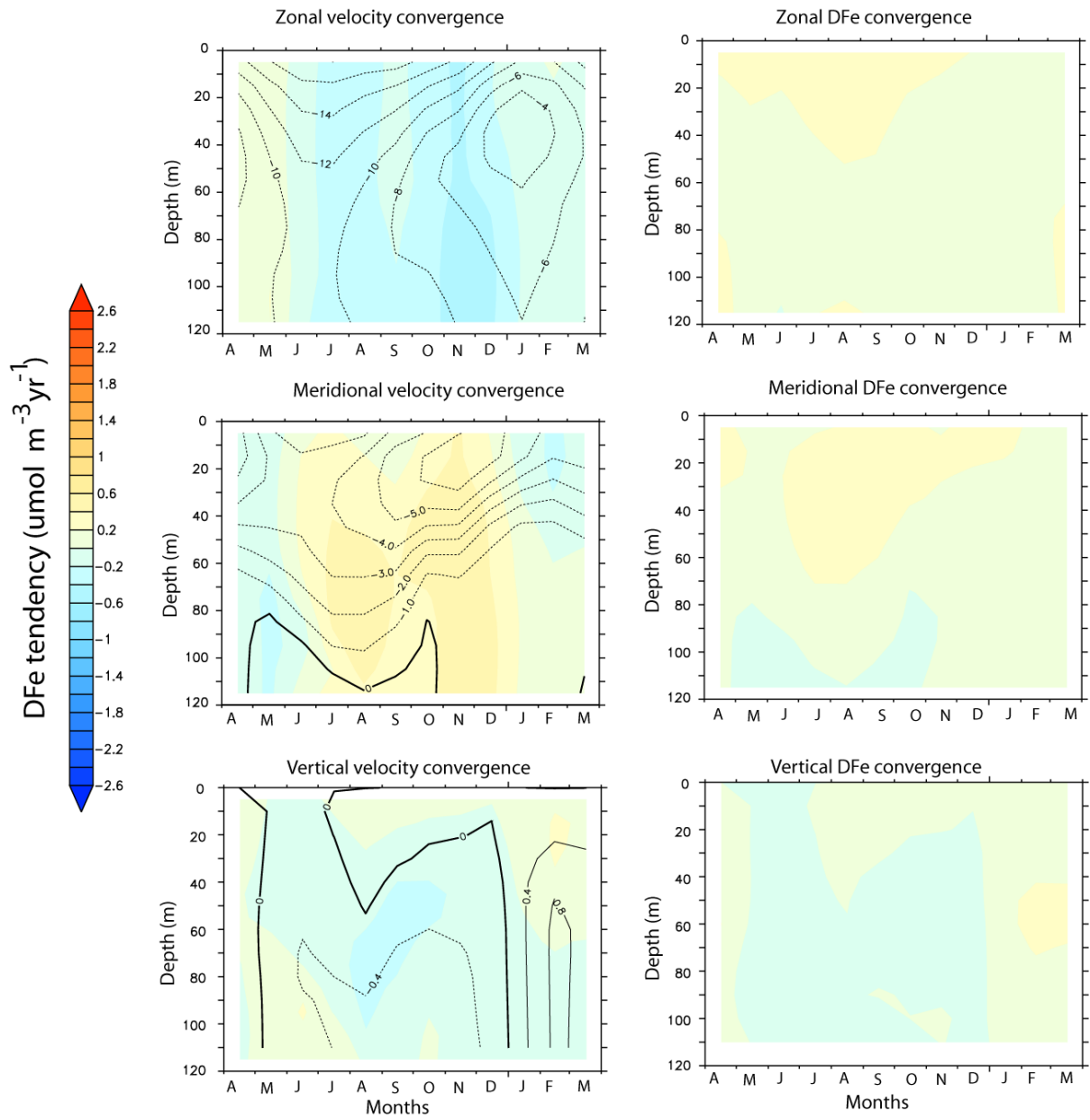


Fig. S15 Same as Figure S12 but for the central southern tropical IO.

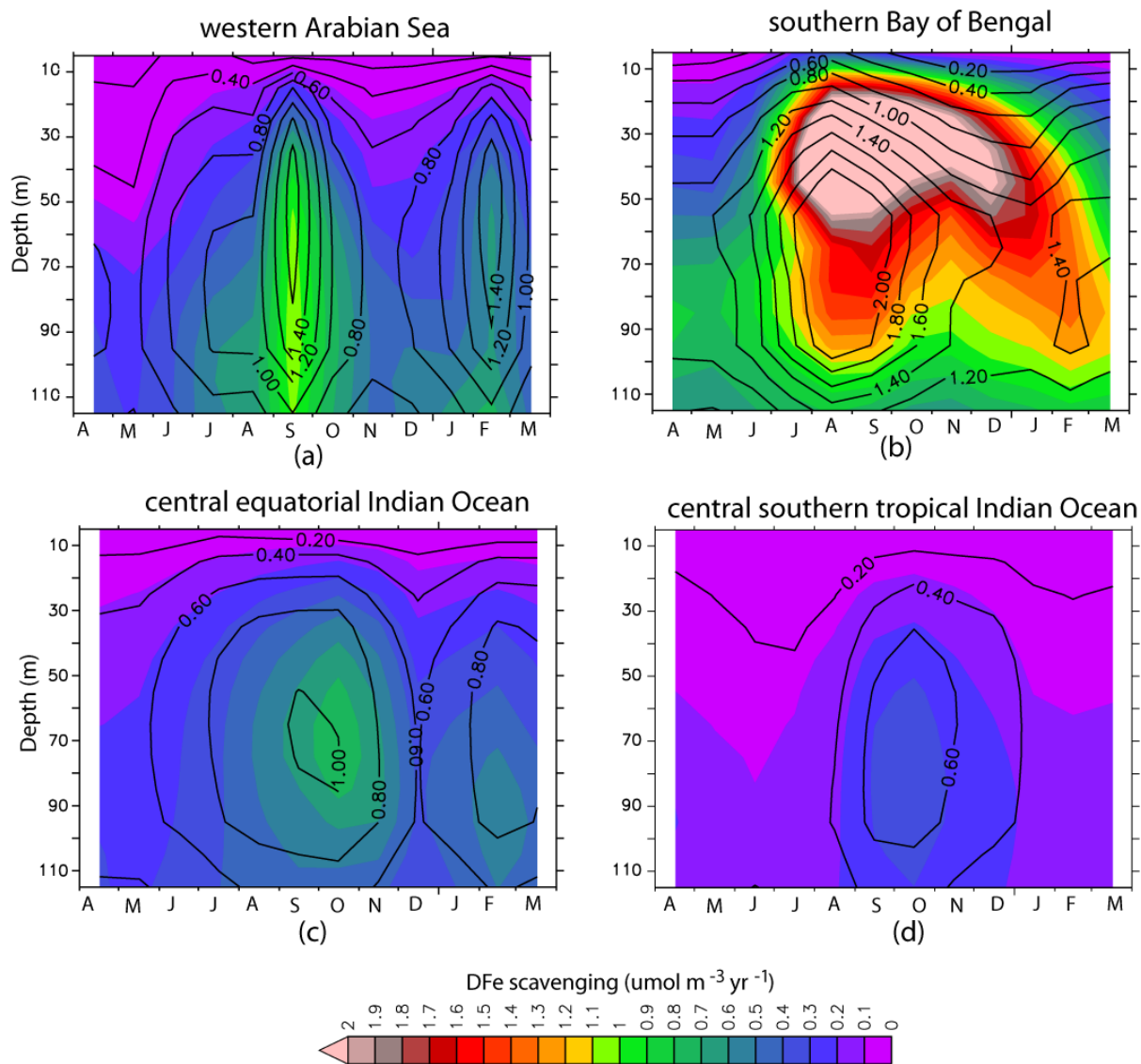


Fig. S16 Shading indicates the variation of DFe scavenging ($\mu\text{mol m}^{-3} \text{yr}^{-1}$) with time and depth for the 4 regions described in Figure 9. The contours represent particulate iron remineralization ($\mu\text{mol m}^{-3} \text{yr}^{-1}$) for these regions.

References

Holte, J., Talley, L. D., Gilson, J., and Roemmich, D.: An Argo mixed layer climatology and database, *Geophys. Res. Lett.*, 44, 5618–5626, <https://doi.org/10.1002/2017GL073426>, 2017.